J. Opt. A: Pure Appl. Opt. **9** (2007) S256–S263 doi:10.1088/1464-4258/9/8/S20

Brownian motion in a modulated optical trap

Yi Deng, John Bechhoefer and Nancy R Forde

Department of Physics, Simon Fraser University, 8888 University Drive, Burnaby, British Columbia, V5A 1S6, Canada

E-mail: bechhoef@sfu.ca and nforde@sfu.ca

Received 27 December 2006, accepted for publication 26 January 2007
Published 25 July 2007
Online at stacks.iop.org/JOptA/9/S256

Abstract
Motivated by recent attempts to use parametric resonance to calibrate the spring constant of a Brownian particle in an optical trap, we have looked systematically at the effects of modulating laser power on the motion of the trapped particle. We predict and find experimentally an increase in the particle's position variance at low laser modulation frequencies, but we find no evidence for any resonant effects in the extremely overdamped motion of the trapped particle. Our results can serve as a guide for designing multiple traps by the 'time-sharing' method.

Keywords: optical tweezers, Brownian motion, trap modulation, variance, time-sharing tweezers

(Some figures in this article are in colour only in the electronic version)

1. Introduction

Over the past twenty years, the technique of optical tweezers has found wide application in the measurement of forces on single molecules and materials in physical and biophysical studies [1, 3]. The relation between force and displacement for a trapped object depends on several parameters: the size, shape and index of refraction of the trapped object; the wavelength and power of the trapping laser; the numerical aperture of the focusing objective, etc [3, 4]. In the small-displacement regime, the particle–trap interaction is approximately that of a harmonic potential, with a force–displacement coefficient called the *trap stiffness* or, more loosely, *spring constant*. To determine the trap stiffness experimentally, one can measure directly the displacement produced by a known external force—for example, the Stokes drag in a constant flow [5–7] or associated with the fluid flow produced by an oscillatory motion of the surrounding solution [2]. An alternate method analyses the random forces of thermal fluctuations by looking at the variance or the power spectrum of position [8]. While the naive application of such methods produces results that are accurate to 10–20%, more refined analyses that consider nonlinearities in the trapping potential and boundary-layer hydrodynamics can increase the accuracy ten-fold [8]. Combining the two methods (viscous drag and power spectrum) eliminates the need to estimate the hydrodynamic drag coefficient, a persistent potential source of systematic error [9].

Recently, Joykutty *et al* attempted to develop a new method for calibrating the stiffness of an optical trap that was based on the periodic modulation of trap stiffness [10]. While there are serious difficulties with that technique [11, 12], the effects of a modulated trap have both fundamental and practical interest, and we focus on these aspects in this paper. In an underdamped mechanical system, the periodic temporal modulation of trap stiffness can lead to parametric resonance [13]. Brownian motion in such systems is relevant to atoms in magneto-optical traps and has been studied both theoretically [14] and experimentally [15, 16]. Under the proper conditions, trap modulation can lead to an increase in damping and a decrease in the variance of positional fluctuations of the Brownian particle. Such a decrease corresponds to a 'cooling' of the 'temperature' of the trapped particle and is a desired feature of such traps. On the other hand, parametric excitation can also lead to an instability (Hopf bifurcation), where the motion of the particle increases exponentially [17]—an undesirable result. Thus, a full understanding of the effects of modulation is important in such cases.

Here, the system of interest is a small colloidal particle in a viscous fluid. The motion is extremely overdamped, with dimensionless dampings that are typically $\mathcal{O}(10)$. (The dimensionless damping is one for a critically damped system.)

As we shall see, in the overdamped limit, parametric modulation does not lead to the resonant effects seen in underdamped systems; however, in the low-frequency limit, we shall see that modulation does increase the variance of the particle's motion. There are practical consequences to this effect, as there are a number of situations of recent interest where the trap stiffness is indeed modulated. For example, in time-sharing optical traps, the direction of the trapping beam is switched among several angles to create multiple traps [7]. For each trap, the power turns on and off periodically, a temporal modulation. In another example, linear-scanning optical tweezers [18] create a constant force optically. In this technique, the potential is modulated both spatially and temporally. Finally, there is an alternative method for creating multiple traps based on spatial light modulators that use holographic gratings to deflect the beam [19]. Here, some of the commercial modules produce an (undesired) intensity modulation at a frequency ≈100 Hz [20]. In all these cases, the increase in variance produced by modulation is an undesired effect. While simple arguments show that modulating the trap strength at frequencies greater than the particle's response frequency ensures that its stiffness may be safely approximated by its time-averaged value [7], our work here will investigate experimentally and theoretically the consequences of modulating at a lower frequency.

Specifically, in this work, we experimentally measure the variance of the position of a trapped object in a modulated optical trap and compare the result with the predictions of a simple theory based on the overdamped Brownian motion of a particle in a parametrically modulated harmonic trap. In section 2, we introduce a theory for calculating position variances that does not assume large damping and then take the overdamped limit. In section 3, we describe our experimental implementation of a modulated trap. In section 4, we discuss our findings, with the aim of providing intuitive interpretations of the results.

2. Model description and theory

In this section, we introduce the equation of motion of an optically trapped bead in a modulated harmonic potential. We focus on the particle's position variance and discuss its behaviour in both high- and low-modulation frequency limits.

In an optical trap, the interaction between the laser and the trapped object can be approximated by a harmonic potential. In such a case, the equation of motion for the trapped bead is given by the Langevin equation,

$$m\ddot{x} + \gamma_0\dot{x} + \kappa x = \sqrt{2k_BT\gamma_0}\,\eta(t). \tag{1}$$

Here, m is the mass of the bead, x its position, κ the trap stiffness, γ_0 the drag coefficient (friction coefficient), k_BT the thermal energy and $\eta(t)$ a stochastic Gaussian process satisfying

$$\langle\eta(t)\rangle = 0; \tag{2}$$

$$\langle\eta(t)\eta(t')\rangle = \delta(t-t'). \tag{3}$$

The drag coefficient γ_0 is well approximated by a constant determined by Stokes' Law,

$$\gamma_0 = 6\pi\rho\nu r, \tag{4}$$

where ρ is the density of the surrounding fluid, ν its kinematic viscosity and r the radius of the trapped spherical object. Hydrodynamic effects introduce high-frequency corrections to (1) that we neglect [8][1].

Since a micron-sized bead optically trapped in an aqueous environment is a highly overdamped system, the inertial term can be dropped from (1), leaving

$$\gamma_0\dot{x} + \kappa x = \sqrt{2k_BT\gamma_0}\eta(t). \tag{5}$$

From this equation of motion, the expected value of the power spectrum density of the position of the trapped bead is given by a Lorentzian [8]:

$$\langle P(f)\rangle = \left(\frac{1}{2\pi^2}\right)\frac{k_BT/\gamma_0}{(f_c^2+f^2)}. \tag{6}$$

Here $P(f)$ is the power density at frequency f and $f_c = \kappa/(2\pi\gamma_0)$ is the corner frequency (also called the particle's response, or roll-off frequency). Fitting the experimental power spectrum to (6) or to improved models [8] thus provides a value for the trap stiffness. In this method, errors in bead-size measurement and fluid viscosity will directly affect the trap stiffness estimate. This problem is partly solved in [8].

If the trap stiffness is modulated sinusoidally, the overdamped equation of motion becomes

$$\gamma_0\dot{x} + \kappa[1+\epsilon\cos(\Omega t+\phi)]x = \sqrt{2k_BT\gamma_0}\,\eta(t), \tag{7}$$

where ϵ is the modulation depth, Ω the modulation frequency and ϕ the initial phase. In experiments, this initial phase is usually unknown and evenly distributed between 0 and 2π. In our linear dissipative system (7), information about the initial conditions decays exponentially and thus does not affect the asymptotic behaviour; since we are only interested in the latter, we can set the initial phase to 0.

The position variance of the trapped bead $\sigma_{xx}(t)$ satisfies (see appendix A for derivation)

$$\dot{\sigma}_{xx}(t) = 2\left[\frac{k_BT}{\gamma_0} - \frac{\kappa}{\gamma_0}(1+\epsilon\cos\Omega t)\sigma_{xx}\right]. \tag{8}$$

When $\epsilon \ll 1$, the approximate solution of (8) gives a Lorentzian form for the variance as a function of modulation frequency [11]. There is no analytical solution to (8) for arbitrary ϵ.

We examine the behaviour of (8) in the limit of high and low Ω for insight into how the frequency of modulation affects the position variance of the trapped bead. The solution of (8) can be written in integral form as

$$\sigma_{xx}(t) = \frac{k_BT}{\kappa} - \frac{2k_BT\epsilon}{\gamma_0}e^{-\frac{2\kappa}{\gamma_0}[t+\frac{\epsilon}{\Omega}\sin\Omega t]} \times \int_0^t e^{\frac{2\kappa}{\gamma_0}[\tau+\frac{\epsilon}{\Omega}\sin\Omega\tau]}\cos\Omega\tau\,d\tau, \tag{9}$$

where we have assumed that initially σ_{xx} has the equilibrium value given by the equipartition theorem, k_BT/κ.

[1] Strictly speaking, for our system of a trapped bead in fluid, the mass term appearing in (1) is an effective particle mass depending on frequency, and the drag coefficient is also frequency-dependent. At the frequencies considered here, however, the inertial term is negligible and it is a good approximation to treat the drag coefficient γ as constant. For ease of comparison with other systems, we include the inertial term in (1), and subsequently drop it for detailed analysis of our overdamped system.

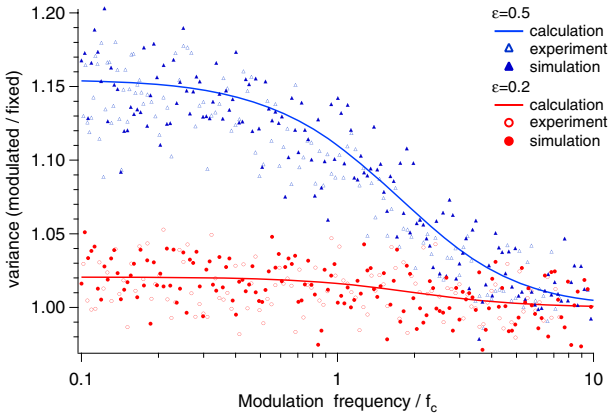

Figure 1. Position variance plotted as a function of modulation frequency Ω, at two different modulation depths, $\epsilon = 0.2$ (circles) and 0.5 (triangles). The predictions from (9) are shown as solid lines, with Monte Carlo simulations (closed symbols) and experimental data (open symbols) superposed. The transition from low- to high-frequency limits ($k_B T/(\kappa\sqrt{1-\epsilon^2})$ to $k_B T/\kappa$) occurs at the corner frequency, f_c.

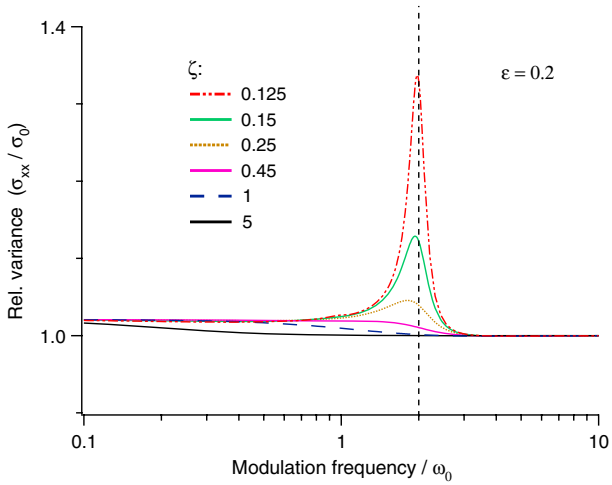

Figure 2. Numerical solution to (A.9) for the position variance in the vicinity of critical damping, for a modulation depth $\epsilon = 0.2$. The variances are relative to the unmodulated equilibrium value. The damping factor $\zeta \equiv \gamma_0/2\sqrt{m\kappa}$ is used to characterize the damping strength. In the low damping regime, a parametric resonance peak is shown clearly near $2\omega_0$. As the damping increases beyond critical damping, the resonance peak quickly vanishes.

In the limit of fast modulation $\Omega \gg f_c$, (9) is Taylor expanded to

$$\sigma_{xx}(t) = \frac{k_B T}{\kappa} - \frac{2k_B T\epsilon}{\gamma_0 \Omega}(\sin \Omega t) + \mathcal{O}\left(\frac{1}{\Omega^2}\right). \tag{10}$$

For fast modulation, the asymptotic spatial variance oscillates around the equilibrium value sinusoidally with a magnitude proportional to $1/\Omega$. The solution approaches the equilibrium value as Ω increases:

$$\sigma_{xx|\Omega\to\infty} = \frac{k_B T}{\kappa}. \tag{11}$$

This system, with corner frequency f_c, can respond only to perturbations slower than f_c. The trapped bead experiences only the average trap stiffness in this case of high-frequency modulation.

In the limit of slow modulation $\Omega \ll f_c$, $\dot{\sigma}_{xx}$ in (8) vanishes adiabatically, and

$$\sigma_{xx|\Omega\ll f_c} = \frac{k_B T}{\kappa(1+\epsilon\cos\Omega t)}. \tag{12}$$

The result in (12) can be obtained intuitively by noting that if the trap stiffness is modulated as $\kappa(1+\epsilon\cos\Omega t)$, with a modulation frequency much lower than the corner frequency, the motion of the bead is always governed by the instantaneous trap stiffness. The average variance over one period is

$$\langle\sigma_{xx}\rangle_{\Omega\ll f_c} = \frac{k_B T}{\kappa}\frac{\Omega}{2\pi}\int_0^{2\pi/\Omega}\frac{\mathrm{d}t}{1+\epsilon\cos\Omega t} = \frac{k_B T}{\kappa\sqrt{1-\epsilon^2}}. \tag{13}$$

Compared with the cases of fast or no modulation, the variance increases for slow modulation with an experimentally detectable factor, $1/\sqrt{1-\epsilon^2}$. The transition between these two limiting cases (11) and (13) is governed by f_c, since the overdamped system has only one timescale, $1/f_c$ [11].

We solved (8) numerically to show the relation between position variance and modulation frequency for the overdamped system (figure 1, solid lines). In the limit of slow modulation, the variance is increased relative to a trap of constant stiffness κ by a factor of $1/\sqrt{1-\epsilon^2}$. As the modulation frequency increases beyond the corner frequency, the variance approaches that of an unmodulated trap because the system is not able to respond faster than the corner frequency f_c.

To further test the analysis, we also performed Monte Carlo simulations of (7), using parameters to match the experiments described below. Figure 1 (closed symbols) demonstrates that the relation between modulation frequency and Brownian motion from the simulations agrees with the numerical solution to (8).

In the more general case including inertial effects, fluctuations are described by a symmetric two-by-two covariance matrix for σ_{xx}, σ_{xv} and σ_{vv}, where v represents velocity. The time evolution of the covariance matrix was derived in [14] (and, by slightly different means, in appendix A, below). Here, we integrate the solution numerically to show that parametric resonance [13] vanishes when the stochastic system goes from under- to overdamped (figure 2). The value of the damping factor $\zeta \equiv \gamma_0/2\sqrt{m\kappa} = \omega_0/4\pi f_c$ is set to several values near 1 and the asymptotic stationary solution of the covariance matrix (A.6) is solved and averaged over one period. (Here, $\omega_0 = \sqrt{m/\kappa}$ is the natural frequency of the system if underdamped.) The result shows a damped parametric resonance peak vanishing as the damping factor increases. In a typical optical tweezers set-up where a 2 μm diameter polystyrene bead is trapped by a 100 pN μm^{-1} optical trap, the dimensionless damping factor is $\mathcal{O}(10)$. An increase in the variance near $2\omega_0$ due to parametric modulation is thus not expected.

To summarize: from the stochastic equation of motion, we have derived the dynamics of the covariance matrix and

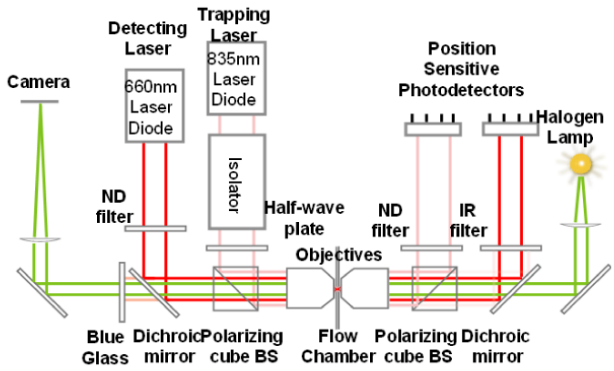

Figure 3. The optical trapping set-up used in these experiments. A near-infrared laser (light pink) is used for trapping (835 nm, 200 mW diode from JDS Uniphase; laser assembled by Melles Griot). A Faraday isolator (Optics for Research Inc., IO-10-834-LP) protects the laser from backscattered light. A red laser (660 nm, 30 mW, Circulase diode laser from Blue Sky Research) measures the position of a trapped bead by back-focal-plane detection using a position-sensitive photodetector (UDT Sensors DL-10). The trapping laser current is controlled by a laser driver (Melles Griot 06DLD203A) driven by a computer-controlled function generator (Stanford Research Systems DS345). We used identical lenses (Olympus UPlanApo/IR, NA 1.2, 60×, water immersion) for trapping and for collecting the scattered light for position detection. Abbreviations used in the figure: ND filter—neutral density filter; IR filter—infrared filter; BS—beam splitter.

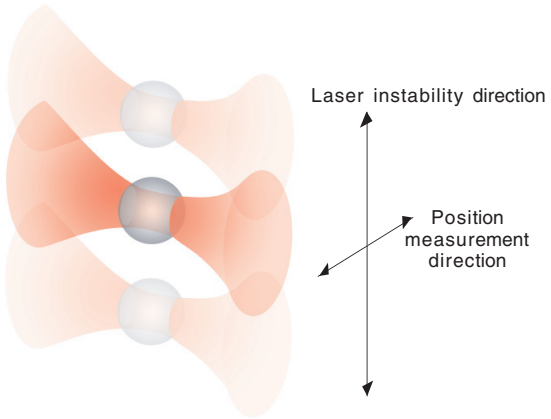

Figure 4. Sketch showing the (exaggerated) effect of the pointing instability of the trapping laser diode. The vertical motion creates a periodic force that modulates the vertical position of the particle. Because of the linearity of the equations of motion, displacements in the orthogonal, horizontal direction are unaffected. We thus rotated the position detector to align its vertical axis with the modulated motion of the bead and recorded positions along the orthogonal direction.

calculated the variance of the position signal. The variance has different behaviour in the low- and high-modulation-frequency limits, leading to a transition in variance near the corner frequency.

3. Experimental approach

To experimentally test the above theoretical results, we trapped a polystyrene bead in an optical tweezers instrument and modulated the trap strength. We determined the variance as a function of modulation frequency and compared the result with our theory.

We performed these experiments on a position-measuring optical tweezers set-up with a single trap (figure 3). The 835 nm light from a 200 mW diode laser was focused by an objective lens into a flow chamber to trap a 2.1 μm polystyrene bead (Spherotech). The forward-scattered light was collected by an identical objective lens. The position of the trapped bead can be obtained by back-focal-plane detection of the trapping laser light on a position-sensitive photodetector. In order to change the trap stiffness, we directly modulated the driving current with a laser driver via a computer-controlled function generator. Because the trapping laser is modulated and because the output signal from the photodetector and its associated amplifier depends on the intensity of the light, we added a weaker, unmodulated laser and detector to perform position detection in these experiments. The whole set-up was enclosed in a plastic shield to reduce laser beam deflection due to air currents [21].

In these experiments, we modulated the laser current about a mean value that corresponded to a characteristic bead corner frequency near 400 Hz. This frequency was in the middle (logarithmically) of a range defined, on the low end, by drifts limiting sampling lengths to $\lesssim$0.1 s and, on the high end, by the bandwidth of the laser modulation driver (10 kHz). Using the intensity of the trapping laser as read by its photodetector, we set the chosen modulation depths to 1% accuracy.

In addition to modulating the laser intensity, varying the current also led to a small ($\approx$100 nm) shift in the central position of the optical trap depending on the intensity (see appendix B). Although this gave a large spurious contribution to the position variance, we realized that the beam modulation was always along one direction. Because of the linearity of the equation of motion (7), the effect of this spatial modulation was minimized by measuring position fluctuations along the orthogonal direction. To do this, we rotated the photodetector so that the spurious motion was along one axis of the detector (the vertical axis in figure 4). This decoupling procedure eliminated the spatial modulation along the orthogonal axis and allowed us to study the system in this one dimension. This method is valid only if the system dynamics is linear and the pointing instability is one dimensional, which were both true in our case.

The corner frequency was determined from the power spectrum method [8] to be 393 $\pm$ 3 Hz (figure 5), and the modulation frequency was chosen to range from 30 Hz to 3 kHz. For each modulation frequency, we recorded a series of 100 position–time measurements, each sampled at 30 kHz for 0.1 s. After each series of measurements at a given modulation frequency, we recorded an identical control series without modulation.

We took the control measurements because of the low-frequency drifts in measured positions referred to above. The drifts had two principal sources: temperature changes in the apparatus that changed beam directions and hops between laser modes in the detecting laser. The latter introduced a positive error in the variance measurement, and the magnitude of this error drifted over large timescales. (Because these shifts were in the measurement laser, they did not affect the actual position of the trapped bead.) By comparing the variance

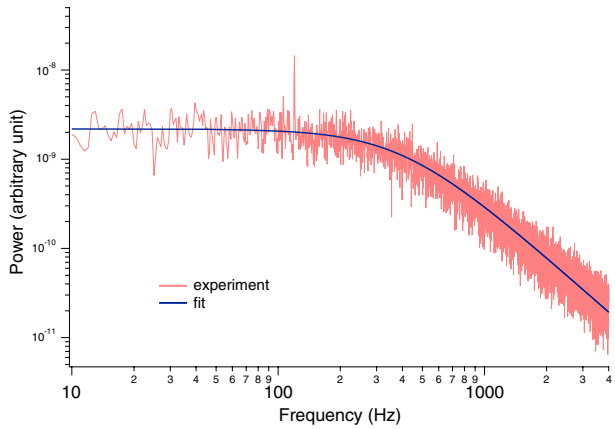

Figure 5. Power spectrum of the trapped bead (2.1 μm, polystyrene), as measured by the main trapping laser with unmodulated, constant power (≈30 mW at the trap). The solid line is a fit to a modified Lorentzian (equation (34) of [8]) and gives a corner frequency of 393 ± 3 Hz. The peak at 120 Hz is from mechanical vibrations and was filtered out prior to fitting. The power spectrum obtained using the red detecting laser gave the same corner frequency (data not shown).

with modulation to a variance calculated from averaged data from an unmodulated trap taken immediately before and afterward, we eliminated these sources of systematic error. As a consequence, the data in figure 1 show ratios of modulated to unmodulated variances.

We calculated the variances of each 100 modulated and control position–time series for each modulation frequency and median-filtered these 100 variances. Because variances are always positive, measurement errors are always biased to positive values, and occasional large external noise (other beads flowing by the beam path, large mechanical vibrations, etc) can overwhelm the Brownian motion signal. A median filter thus gives a better estimate of the true relative variance than does an averaging filter. Figure 1 shows the normalized experimental variance obtained as a function of modulation frequency. The numerical simulation data and theoretical calculations, which use the same parameters as in the experiments, are also included. All results are consistent and show that, at low frequencies, the relative variance asymptotically approaches $1/\sqrt{1-\epsilon^2}$, with a transition frequency equal to the corner frequency. Notice that the scatter in the variance measurements is consistent with the scatter in the Monte Carlo simulations, showing that we have correctly modelled not only the physics of the trapped bead but also the statistics of the experimental measurements.

4. Discussion

The focus of our study was to determine how the position variance of an optically trapped object is affected by a temporally modulated trap intensity. We found that, at low modulation frequencies, the variance with modulation is higher by a factor of $1/\sqrt{1-\epsilon^2}$, where ϵ is the depth of modulation. In the high-frequency limit, the variance is governed by the time-averaged stiffness of the optical trap and equals the variance without modulation. The transition between these two limiting cases occurs on the timescale of viscous relaxation, which is related to the corner frequency. We show theoretically, numerically and experimentally that the transition frequency indeed occurs around the corner frequency for different modulation depths.

In principle, the dependence of the variance on modulation frequency could be used to calibrate an optical trap. Earlier work by Joykutty *et al* noted a peak in the variance as a function of modulation, which they interpreted as a resulting from parametric resonance [10]. If true, this would enable a precise determination of the trap stiffness, as the observed peak is sharp. However, the theoretical arguments presented here and in [11] imply that no such peak is expected in a highly overdamped system. In addition, a careful scan of the variance near the expected frequency ($2\omega_0$) in our system showed no such peak [12]. The result of Joykutty *et al* is thus due to other unknown causes. Nonetheless, the observed relations between variance and modulation frequency are characterized by the trap stiffness (figure 1), and thus experimentally determining this relation should enable determination of the trap stiffness. However, the absence of an analytical form for the variance-modulation relation, the long sampling time and experimental subtleties make it hard to obtain an accurate and convenient corner frequency measurement. The power spectrum analysis method, which uses all the information in the position signal, remains the best calibration method.

Although the dynamics in the overdamped regime are less rich than in an underdamped system [15–17], the frequency dependence of the measured variance nonetheless has important implications for experimental design. Because there is only one timescale in overdamped systems, the corner frequency also sets the timescale for modulation in instruments such as time-sharing optical tweezers [7]. When controlled by an acousto-optic deflector, the modulation frequency is usually on the scale of kHz or higher, depending on the size of the modulator and number of traps [7]. Effectively, the trapped bead acts as a low-pass filter for the modulation. So long as the modulation frequency is much higher than the corner frequency, the variance is independent of the specific waveform of modulation. In such an application, the effect of modulation can be neglected, and each trap can be treated as having a constant trapping strength given by the time-averaged intensity at each trap. Here, it is also valid to treat the force–displacement relation as linear. When controlled by a rotating mirror, by contrast, the modulation is much slower [2, 22–24], and the position variance of isolated trapped beads can be time-dependent, with a time-averaged value higher than when trapped by a constant-power trap. In this case, the optical trap should only be used as a tool to move objects. Since the force–displacement relation depends on the details of modulation (frequency, duty cycle, etc), quantitative measurements will be highly susceptible to systematic errors. As the modulation amplitude increases close to $\epsilon = 1$ (full on/off modulation), the relation between variance and modulation frequency becomes increasingly ill fit by a Lorentzian, with the variance diverging at low frequencies; however, the high-frequency behaviour is independent of modulation depth, converging to variance of a time-averaged trap at frequencies greater than $10\,f_c$. Therefore, for quantitative analysis, the modulation frequency should be at least an order of magnitude above the corner frequency.

In many biophysical applications, optical tweezers are used to probe the mechanical properties of biological systems. In such applications, the trapped bead is in contact with or tethered to a soft molecule or material. This can result in a decrease of the viscous relaxation time of the bead because of the elasticity of the attached molecule, effectively increasing the corner frequency [7]. In such a case, a time-sharing trap that gives reliable quantitative results on isolated beads may nonetheless give systematic errors when applied to force measurements on materials. Additionally, in this type of experiment, an external force applied to the trapped bead results in a displacement from the trap centre, and thus modulation of the trap stiffness will induce an oscillation of the bead's position. Under certain conditions this oscillation amplitude can exceed the Brownian motion, which has implications when characterizing force-dependent systems such as molecular motors. Therefore, care must be taken when using time-sharing traps for force-sensitive studies.

Another reason to modulate the trap stiffness in optical tweezers is to actively control the trap stiffness in order to create a constant-force trap or a position controller [25]. The constant-force trap (force clamp) is useful in biophysical and biochemical studies, in which a controllable force load can be used to probe systems such as molecular motors, nucleic acids and protein folding, and to measure statistics in near- and non-equilibrium systems [26]. Besides active intensity modulation, other ways to create a force clamp include laminar fluid flow [5, 6, 27, 28], active position feedback [29, 30], scanning the trap centre with a changing trap strength [18], and taking advantage of the anharmonic trapping potential [31]. Most of these other techniques require expensive modulators such as acousto-optic deflectors or high-resolution positioning stages, whereas intensity modulation can be performed cheaply by modulating the current of a laser diode. Also, when used for position control, although closed-loop feedback does not increase the signal-to-noise ratio of force measurements, physically reducing the Brownian motion can nonetheless be useful. For example, for studies on short molecules, reducing the Brownian motion can decrease unwanted contributions from interactions between closely spaced beads. Also, since many theoretical arguments are more simply framed in terms of a constant-force constraint, comparisons between experiment and theory are simplified by measurements in which the force is held fixed [32]. The frequency response of the variance discussed in our study suggests that the closed-loop feedback bandwidth must exceed the corner frequency in order to effectively control the signal or force in the face of perturbations due to thermal noise.

5. Conclusion

In a typical optical tweezers set-up, the corner frequency, proportional to the trap stiffness, is the relevant timescale for the system. We observed experimentally that, if the laser intensity is modulated sinusoidally, the variance of the position of the trapped object increases by a factor of $1/\sqrt{1-\epsilon^2}$ in the low-modulation-frequency limit and the transition takes place around the corner frequency. In principle, this variance-modulation frequency dependence could be used to calibrate an optical trap; however, the standard power spectrum method is better, being more accurate, faster and requiring less hardware. On the other hand, we have shown that low modulation frequencies do lead to detectable increases in the position variance, and we have confirmed the expected form of the increase. Such variances can lead to systematic errors in force measurements from time-varying traps, and we have given criteria for avoiding such effects.

Acknowledgments

We thank Philip Johnson for discussions and help with instrument construction. We acknowledge financial support from NSERC Canada (JB and NRF) and the Michael Smith Foundation for Health Research (NRF).

Appendix A. Time evolution of the variance

The central results in our analysis are based on the equations of motion for the time evolution of the position variance for a Brownian particle in a parametrically modulated harmonic trap with arbitrary damping. Those equations were first derived by Zerbe *et al* [14]. Here, we give an alternate derivation for the overdamped case and discuss briefly how to extend it to the more general arbitrary damping case.

For the overdamped equation of motion,

$$\gamma_0 \dot{x} + \kappa[1 + \epsilon\cos(\Omega t + \phi)]x = \sqrt{2k_B T\gamma_0}\,\eta(t), \qquad \text{(A.1)}$$

we define the diffusion constant of the bead to be $D = k_B T/\gamma_0$ and scale t using the corner frequency $t' = 2\pi f_c t$. The overdamped equation of motion then simplifies to

$$\dot{x} + \left[1 + \epsilon\cos\left(\frac{\Omega}{2\pi f_c}t' + \phi\right)\right]x = \sqrt{\frac{2D}{2\pi f_c}}\eta(t'). \qquad \text{(A.2)}$$

The equivalent stochastic differential equation is

$$\mathrm{d}x = -\left[1 + \epsilon\cos\left(\frac{\Omega}{2\pi f_c}t' + \phi\right)\right]x\,\mathrm{d}t' + \sqrt{\frac{2D}{2\pi f_c}}\,\mathrm{d}w(t'), \qquad \text{(A.3)}$$

where $w(t')$ is a Wiener process [33]. Following the derivation of Itō's lemma [33, 34],

$$\begin{aligned}\mathrm{d}(x^2) &= 2x\,\mathrm{d}x + (\mathrm{d}x)^2 \\ &= -2\left[1 + \epsilon\cos\left(\frac{\Omega}{2\pi f_c}t' + \phi\right)\right]x^2\,\mathrm{d}t' \\ &\quad + 2\sqrt{\frac{2D}{2\pi f_c}}x\,\mathrm{d}w\,(t') + \frac{2D}{2\pi f_c}\,\mathrm{d}w^2(t') \\ &= 2\left[-\left[1 + \epsilon\cos\left(\frac{\Omega}{2\pi f_c}t' + \phi\right)\right]x^2 + \frac{D}{2\pi f_c}\right]\mathrm{d}t' \\ &\quad + 2\sqrt{\frac{2D}{2\pi f_c}}x\,\mathrm{d}w(t'), \end{aligned} \qquad \text{(A.4)}$$

since $\mathrm{d}w^2 = \mathrm{d}t'$ and we neglect terms of higher order than $\mathrm{d}t'$. For a continuous function $f(x)$ of $x(t')$, Itō's lemma also

implies $\mathrm{d}\langle f(x)\rangle = \langle \mathrm{d}f(x)\rangle$ [33]. Thus, since $\langle x\rangle = 0$, and $\langle x(t')\,\mathrm{d}w(t')\rangle = 0$, the position variance $\sigma_{xx} = \langle x^2\rangle$ is

$$\begin{aligned}\mathrm{d}\sigma_{xx}(t') &= \mathrm{d}\langle x^2(t')\rangle \\ &= \langle \mathrm{d}x^2(t')\rangle \\ &= 2\left[-\left[1+\epsilon\cos\left(\frac{\Omega}{2\pi f_\mathrm{c}}t'+\phi\right)\right]\langle x^2(t')\rangle + \frac{D}{2\pi f_\mathrm{c}}\right]\mathrm{d}t',\end{aligned} \tag{A.5}$$

or

$$2\pi f_\mathrm{c}\dot{\sigma}_{xx}(t') = 2\left[D - \frac{\kappa}{\gamma_0}\left[1+\epsilon\cos\left(\frac{\Omega}{2\pi f_\mathrm{c}}t'+\phi\right)\right]\sigma_{xx}\right]. \tag{A.6}$$

In unscaled units, (A.6) becomes (8).

In the full second-order stochastic system,

$$\frac{m\kappa}{\gamma_0^2}\ddot{x}+\dot{x}+\left[1+\epsilon\cos\left(\frac{\Omega}{2\pi f_\mathrm{c}}t'+\phi\right)\right]x = \sqrt{\frac{2D}{2\pi f_\mathrm{c}}}\eta(t'), \tag{A.7}$$

where the factor $\gamma_0^2/m\kappa = (\omega_0/2\pi f_\mathrm{c})^2 = 4\zeta^2$ is used to characterize the strength of damping. In our case, this quantity is $\mathcal{O}(10^2)$. To determine the variance of the motion of the trapped bead, we use the covariance matrix [14],

$$\begin{aligned}\sigma(t) &= \begin{pmatrix}\sigma_{xx}(t) & \sigma_{xv}(t)\\ \sigma_{xv}(t) & \sigma_{vv}(t)\end{pmatrix} \\ &= \begin{pmatrix}\langle x^2\rangle - \langle x\rangle^2 & \langle xv\rangle - \langle x\rangle\langle v\rangle \\ \langle xv\rangle - \langle x\rangle\langle v\rangle & \langle v^2\rangle - \langle v\rangle^2\end{pmatrix}.\end{aligned} \tag{A.8}$$

Following a derivation similar to that used for the first-order system, one can show that the stochastic system described in (A.7) leads to the following dynamical equations for the elements of the covariance matrix [14]:

$$\begin{aligned}\dot{\sigma}_{xx} &= 2\sigma_{xv}; \\ \dot{\sigma}_{xv} &= -\frac{\gamma_0^2}{m\kappa}\left[\sigma_{xv} + \left[1+\epsilon\cos\left(\frac{\Omega}{2\pi f_\mathrm{c}}t'+\phi\right)\right]\sigma_{xx}\right] \\ &\quad + \sigma_{vv}; \\ \dot{\sigma}_{vv} &= -2\frac{\gamma_0^2}{m\kappa}\left[\sigma_{vv} + \left[1+\epsilon\cos\left(\frac{\Omega}{2\pi f_\mathrm{c}}t'+\phi\right)\right]\sigma_{xv}\right] \\ &\quad + \frac{2D\gamma_0^2}{m^2(2\pi f_\mathrm{c})^3}.\end{aligned} \tag{A.9}$$

These equations were used to generate the curves in figure 2.

In the overdamped limit, $\gamma_0^2/(m\kappa) = (\omega_0/2\pi f_\mathrm{c})^2 \gg 1$, and the timescales of σ_{xv} and σ_{vv} are much faster than σ_{xx}. We therefore eliminate them adiabatically by setting $\dot{\sigma}_{xv} = \dot{\sigma}_{vv} = 0$ and easily recover (A.6).

Appendix B. Spatial modulation of the trapping laser

In practice, it is easy, when temporally modulating the strength of a laser beam, to also introduce inadvertent positional modulations. The laser beam direction may vary because of effects associated with an external modulator or due to the diode itself. Here, we compare the effects of such positional modulations to those produced by the temporal modulation discussed in the main text.

Consider a sinusoidally moving trap with centre at $x_\mathrm{c} = x_0\cos(\Omega t)$. Transforming the position coordinate to $x' = x - x_\mathrm{c}$, the solution to (7) changes by $x_0\cos(\Omega t) + \mathcal{O}(\epsilon^2)$. Therefore, if the spatial modulation is significant, a sharp peak in the power spectrum is expected at the modulation frequency Ω, with weaker peaks at the harmonics of Ω. To first order, if the position changes linearly with laser intensity and if both position and intensity change sinusoidally with time, the position variance will increase as ϵ^2. Thus, the increase in variance due to spatial modulation resembles that due to intensity modulation (both are $\mathcal{O}(\epsilon^2)$); however, the effects are easily distinguished in the power spectrum, since spatial modulation implies a peak at Ω while intensity modulation gives no peak, in the overdamped case. We also note that spatial modulation is analogous to applying a sinusoidal external force, like that used in the 'shaking stage experiment' to calibrate optical trap stiffness [2]. In any case, as stated in the main text, we minimize spatial modulation in our experiment so that the variance contribution from this artefact is negligible compared with that due to Brownian motion.

References

[1] Lang M J and Block S M 2003 *Am. J. Phys.* **71** 201–15
[2] Hénon S, Lenormand G, Richert A and Gallet F 1999 *Biophys. J.* **76** 1145–51
[3] Neuman K C and Block S M 2004 *Rev. Sci. Instrum.* **75** 2787–809
[4] Rohrbach A 2005 *Phys. Rev. Lett.* **95** 168102
[5] Kuo S C and Sheetz M P 1993 *Science* **260** 232–4
[6] Wuite G J L, Davenport R J, Rappaport A and Bustamante C 2000 *Biophys. J.* **79** 1155–67
[7] Visscher K, Gross S P and Block S M 1996 *IEEE J. Sel. Top. Quantum. Electron.* **2** 1066–76
[8] Berg-Sørensen K and Flyvbjerg H 2004 *Rev. Sci. Instrum.* **75** 594–612
[9] Tolić-Nørrelykke S F, Schäffer E, Howard J, Pavone F S, Jülicher F and Flyvbjerg H 2006 *Rev. Sci. Instrum.* **77** 103101
[10] Joykutty J, Mathur V, Venkataraman V and Natarajan V 2005 *Phys. Rev. Lett.* **95** 193902
[11] Pedersen L and Flyvbjerg H 2007 *Phys. Rev. Lett.* **98** 189801
[12] Deng Y, Forde N R and Bechhoefer J 2007 *Phys. Rev. Lett.* **98** 189802
[13] Landau L D and Lifshitz E M 1976 *Course of Theoretical Physics: Mechanics* 3rd edn (Oxford: Pergamon) section 27
[14] Zerbe C, Jung P and Hänggi P 1994 *Phys. Rev.* E **49** 3626–35
[15] Görlitz A, Weidemüller M, Hänsch T W and Hemmerich A 1997 *Phys. Rev. Lett.* **78** 2096–9
[16] Friebel S, D'Andrea C, Walz J, Weitz M and Hänsch T W 1998 *Phys. Rev.* A **57** R20–3
[17] Kim K, Noh H R, Yeon Y H and Jhe W 2003 *Phys. Rev.* A **68** 031403
[18] Nambiar R, Gajraj A and Meiners J-C 2004 *Biophys. J.* **87** 1972–80
[19] Curtis J E, Koss B A and Grier D G 2002 *Opt. Commun.* **207** 169–75
[20] Dufresne E 2006 personal communication
[21] Abbondanzieri E A, Greenleaf W J, Shaevitz J W, Landick R and Block S M 2005 *Nature* **438** 460–5
[22] Visscher K, Brakenhoff G J and Krol J J 1993 *Cytometry* **14** 105–14
[23] Bronkhorst P J, Streekstra G J, Grimbergen J, Nijhof E J, Sixma J J and Brakenhoff G J 1995 *Biophys. J.* **69** 1666–73
[24] Lenormand G, Hénon S, Richert A, Siméon J and Gallet F 2001 *Biophys. J.* **81** 43–56
[25] Wang M D, Yin H, Landick R, Gelles J and Block S M 1997 *Biophys. J.* **72** 1335–46
[26] Bustamante C, Chemla Y R, Forde N R and Izhaky D 2004 *Annu. Rev. Biochem.* **73** 705–48
[27] Davenport R J, Wuite G J L, Landick R and Bustamante C 2000 *Science* **287** 2497–500

[28] Forde N R, Izhaky D, Woodcock G R, Wuite G J L and Bustamante C 2002 *Proc. Natl Acad. Sci.* **99** 11682–7
[29] Lang M J, Asbury C L, Shaevitz J W and Block S M 2002 *Biophys. J.* **83** 491–501
[30] Liphardt J, Onoa B, Smith S B, Tinoco I and Bustamante C 2001 *Science* **292** 733–7
[31] Greenleaf W J, Woodside M T, Abbondanzieri E A and Block S M 2005 *Phys. Rev. Lett.* **95** 208102
[32] Lubensky D K and Nelson D R 2002 *Phys. Rev.* E **65** 031917
[33] Gardiner C W 1985 *Handbook of Stochastic Methods* 2nd edn (Berlin: Springer) sections 4.2, 4.3
[34] Itō K 1951 *Mem. Am. Math. Soc.* **4** 1–51